

**MULTIPLE SCATTERING ANALYSIS OF
CU-K EXAFS IN $\text{Bi}_2\text{Sr}_{1.5}\text{Ca}_{1.5}\text{Cu}_2\text{O}_{8+\delta}$ ***

J. Röhler[†]

*Universität zu Köln, Physikalisches Institut
D-50937 Köln, Germany*

and

R. Crüsemann

*Universität Stuttgart, Institut für Physikalische Chemie
D-70569 Stuttgart, Germany*

ABSTRACT

We have analyzed the Cu *K*-EXAFS of $\text{Bi}_2\text{Sr}_{1.5}\text{Ca}_{1.5}\text{Cu}_2\text{O}_{8+\delta}$ using a full multiple scattering analysis in a cluster with diameter $d \simeq 7.6$ Å. The layered structure has numerous quasi one-dimensional structural elements which give rise to significant multiple scattering contributions in the EXAFS. We confirm the Sr/Ca ratio of the sample is 1:1, and one Ca atom is located close to a nominal Sr-site. At 40 K the dimpling angle in the CuO_2 -plane is found to be $\leq 3.5^\circ$.

1. Introduction

Knowledge of the positions and the dynamics of the atoms forming the layer between the doping block and the CuO_2 -planes in the high- T_c cuprates is of particular interest for the understanding of their electronic structure and mechanism of superconductivity [1]. The layer contains divalent alkaline-earth atoms (Ba^{2+} , Sr^{2+} , Ca^{2+}) and the apical oxygen. The apical oxygen exhibits many anomalous features: high anisotropic polarizability [2], anharmonic motion, zero contribution to the oxygen isotope effect [3]. Linking the doped CuO_2 planes to the charge reservoir (*N.B.* one-dimensional or quasi-one-dimensional structural Cu-, Bi-, Tl-, or HgO elements [4]), the apical oxygen site is sensitive to the electronic coupling of the 'active' layers, and unusual anharmonicities are expected. The anharmonic potential of the apical oxygen was recently proposed to be of a double well type [5], but so far there is no unambiguous experimental evidence for that special type of anharmonicity [6, 7].

Less attention is attributed to the positions and the dynamics of the alkaline-earth atoms located in the layer between chains and planes. Usually these atoms are considered to act as mere spacers, which adjust their positions dependent on the

*to be published in: Proc. Int. Workshop on "Anharmonic Properties of High- T_c Cuprates", Bled, Slovenia, Sep. 1-6, 1994 (World Scientific).

[†]e-mail: abb12@rs1.rrz.uni-koeln.de

charge redistribution between the electronically active layers. But there is increasing evidence for electron-phonon coupling along the c -axis involving the whole polarizable earth-alkaline–oxygen layer [8].

This contribution deals with the determination of the local structure of the polarizable layer in $\text{Bi}_{2+x}(\text{Sr}, \text{Ca})_3\text{Cu}_2\text{O}_{8+\delta}$ (the 2212 phase) by Cu- K x-ray extended-absorption fine-structure (EXAFS). The photoelectron interference patterns were analyzed using a full multiple scattering calculation up to a total pathlength of 8 Å. Advantageously the 2212 phase exhibits a single Cu site. Therefore interference effects between two local Cu substructures as *e.g.* in $\text{YBa}_2\text{Cu}_3\text{O}_{7-\delta}$ are excluded. But the Bi-cuprates are structurally more complex than the 123 system. For a review see *e.g.* Majewski [9] and references therein.

The 2212 phase exhibits an extended single-phase region with variable Ca, Sr, Bi and oxygen content, which allows considerable variations from the nominal stoichiometric composition $\text{Bi}_2\text{Sr}_2\text{Ca}_1\text{Cu}_2\text{O}_8$. Systematic investigations of the homogeneity range of the 2212 phase confirm the nominal stoichiometric composition is not included in the single-phase region; stoichiometric 2212 samples are always found to contain various secondary Ca–Sr–Bi cuprates. Clearly, contributions from such possible secondary phases superimpose the local structure of the primary phase, and usually there is no reliable procedure to disentangle a complex structural multiphase mixture.

Single-phase materials are therefore a necessary prerequisite for investigations of local, (*i.e.* non translationally invariant) deviations from the average crystallographic structure. Even single-phase optimum doped high- T_c materials, due to their inherent non-stoichiometry, exhibit many vacancies, interstitials or atomic site changes. We have shown recently by EXAFS that oxygen vacancies at the chain ends in single-phase $\text{YBa}_2\text{Cu}_3\text{O}_{7-\delta}$ ($\delta > 0.1$) create two-site apex configurations superimposing possible dynamic double-well anharmonicities [7].

Local structural refinements lacking the constraints due to lattice symmetry appear to be rather complex. Nevertheless, local lattice distortions arising from the inherent nonstoichiometry of the high- T_c cuprates are safely detectable, as well as variations as a function of temperature, provided well characterized single-phase materials have been selected.

2. Experiment

2.1 Sample characterization

T_c of the Bi 2212 phase varies between $\simeq 50$ K and 94 K and is a function of the oxygen, calcium and bismuth content. The critical temperature decreases with increasing Ca and Bi content. In addition a maximum of T_c is observed at a oxygen content $\delta \simeq 0.2$. It is not known, whether the decrease of Ca or Bi content causes directly the increase of T_c , or indirectly by variation of the oxygen content. To our

knowledge the exact composition of optimum doped Bi 2212 is not yet investigated in detail. The sample under investigation (T_c onset: 75 K) has been previously studied by EXAFS using a 'beat' analysis of the filtered Cu–O signal [10]. We had found two different Cu–O1 in-plane bonds differing by $\simeq 0.1 \text{ \AA}$, and the apical bondlength $R_{Cu-O2} = 2.53 \text{ \AA}$. (The present R -space fits are not improved for $R < 2 \text{ \AA}$ by the assumption of split Cu–O1 bonds. Also no improvement of the fits to the tiny $nleg = 2$ bump #2 of the apical oxygen O2 is obtained by variation of its bondlength). The powder x-ray diffraction data exhibit 14 reflections of a single two-layer phase, and three weak superstructure reflections. Reflections of other phases were not detectable. The diffraction data have been refined to the orthorhombic Amma structure with $a \simeq b = 5.4016 \text{ \AA}$ and $c = 30.680 \text{ \AA}$ (300 K) using a profile fit [11]. The variation of the Ca, Sr content has a well determined effect on the c -axis lattice parameter [12]. Using this calibration $c = 30.680 \text{ \AA}$ points to Ca/Sr=1.5:1.5. The superstructure reflections gave $s = 4.78$ for the period of the incommensurate modulation. The Bi and oxygen contents were not determined.

2.2 X-ray absorption measurements and data reduction

The absorption data were recorded with synchrotron radiation at HASYLAB/DESY from a polycrystalline absorber. Special care has been undertaken to avoid texture effects. Useful data could be obtained up to $k = 16 \text{ \AA}^{-1}$. The normalization included the usual energy correction, and a sequence of cubic splines was used to define the high energy background. The oscillations at $R < 1 \text{ \AA}$ visible in the experimental $|\text{FT}(\chi k^2)|$ (Figs. 1,2) are an artefact due to uncertainties in the background definition at low kinetic energies. For maximum resolution the Fourier transform were performed in a rectangular window $k = 3.55 - 16 \text{ \AA}^{-1}$.

3. Experimental Results

3.1 Multiple scattering calculation

The Cu- K EXAFS spectrum of Bi 2212 expected from the average crystallographic structure [13, 14] was calculated in a cluster of 23 atoms using the FEFF 5.05 code [15]. Use of the exact magnetic quantum number expansion developed by [16] yielded identical results [17] which will be presented elsewhere.

Nonequivalent Cu–O1 base bonds were not taken into account. Scattering configurations up to $nleg = 8$ paths with a maximum effective length $R_{eff} = 4 \text{ \AA}$ were allowed. R_{eff} defines half of the total scattering length in a configuration. Setting the amplitude ratio filter to 2.5%, $i = 18$ scattering configurations with $nleg \leq 4$ were selected. $\text{FT}(\chi k^2)$ of the most significant 15 scattering configurations are displayed in Fig. 1 (1–18), and their parameters are listed in Tab. 1. Tab. 1 also displays the parameters resulting from the fit to the experimental data at 40 K shown at the

Table 1. Positions of the atoms in the relevant scattering configurations # exhibited in Fig. 1 where #* are omitted, and #[†] are summed up. The central Cu atom is located at (0, 0, 0). Θ denotes the scattering angle, $180^\circ \equiv$ backscattering, $0^\circ \equiv$ forwardscattering. $nleg$ denotes the number of paths in the scattering configuration, g its degeneracy. σ^2 is a average mean squared displacement. R_{eff} is half of the total scattering length. See text.

#	scatterer	x	y	z	Θ [$^\circ$]	$nleg$	g	rel. amp. [%]	σ^2 [\AA^2]	R_{eff} [\AA]
1	O1	-1.347	1.347	0	180.00	2	4	100.0	0.0043	1.905
2	O2	0	0	2.38	180.00	2	1	14.7	0.0043	1.380
3	Ca1	0	-2.6904	-1.652	180.00	2	4	37.1	0.0060	3.160
4	Ca2	2.694	0	1.661	180.00	2	1	9.1	0.0060	3.165
5	Sr	0	-2.694	1.689	180.00	2	3	26.6	0.0070	3.180
6*						3	8	9.8	0.0043	3.252
	O1	-1.347	1.347	0	135.00					
	O1	1.347	1.347	0	135.00					
7	Cu	0	0	-3.304	180	2	1	6.6	0.0043	3.304
8*						3	8	5.9	0.0043	3.667
	O2	0	0	2.38	141.32					
	O1	1.347	1.347	0	128.68					
9						3	16	5.9	0.0043	3.793
	Ca1	-2.694	0	-1.652	141.93					
	O1	-1.347	1.347	0	90.00					
10*						3	4	3.2	0.0043	3.799
	Ca1	2.694	0	1.661	143.00					
	O1	1.347	1.347	0	90.00					
11	Cu	-2.694	-2.694	0	180.00	2	4	18.7	0.0043	3.810
12						3	8	54.4	0.0043	3.810
	Cu	2.694	-2.694	0	180.00					
	O1	1.347	-1.347	0	0.00					
13 [†]						3	4	16.4	0.0043	3.810
	O1	-1.347	-1.347	0	0.00					
	O1	1.347	1.347	0	180.00					
	O1	1.347	1.347	0	0.00					
14 [†]						4	4	6.6	0.0043	3.810
	O1	1.347	-1.347	0	180.00					
	Cu	0	0	0	180.00					
	O1	1.347	-1.347	0	180.00					
15						4	4	39.4	0.0043	3.810
	O1	1.347	1.347	0	0.00					
	Cu	2.694	2.694	0	180.00					
	O1	1.347	1.347	0	0.00					
16 [†]						4	4	6.3	0.0043	3.810
	O1	1.347	-1.347	0	180.00					
	Cu	0	0	0	0.00					
	O1	-1.347	1.347	0	180.00					
17	O1	1.347	1.347	-3.304	180.00	2	4	17.3	0.0043	3.814
18						3	12	8.9	0.0043	3.815
	Sr	0	-2.694	1.689	143.20					
	O1	1.347	-1.347	90.00	0.00					

top of Fig. 1. The fits have been performed in R -space on visual inspection of the real and imaginary parts of the Fourier transforms. The partial $\chi_i k^2$ were iteratively added in increasing order of their relative amplitude ('rel. amp.' in Tab. 1), Fourier transformed and compared to $|\text{FT}(\chi k^2)|$ of the experimental data. R_{eff} and σ^2 were the only adjustable parameters. After each cycle of the fit, FEFF was completely recalculated using the refined geometry of the cluster as starting condition. The proper choice of σ^2 turned out to be less critical than the choice of the proper atomic configuration, in particular the Sr/Ca ratio, the Cu–O1 dimpling angle, and their precise geometry. Further efforts to optimize the single scattering in the CuO_5 pyramid were not yet made. A larger cluster of 65 atoms turned out to yield the same results as the small cluster of 23 atoms.

3.2 Ca/Sr ratio

Coincidence (although not a fully satisfactory one) between the calculated and the experimental spectra is obtained with the EXAFS from a cluster exhibiting two different Ca-sites: Ca1, Ca2, and a Cu–O1 dimpling angle of 3.5° . The ratio Ca/Sr had to be chosen as 1:1, and the location of Ca2 close to a Sr site, ($\Delta z = -0.028 \text{ \AA}$), with $R_{\text{Cu-Ca2}} = 3.165 \text{ \AA}$. For comparison: $R_{\text{Cu-Ca1}} = 3.160 \text{ \AA}$. The 1:1 Sr/Ca-ratio produces the distinct minimum of $|\text{FT}|$ at $R = 3 \text{ \AA}$, *cf.* Fig. 2. A ratio Ca/Sr 2:1 worsens the fit dramatically, the same occurs for replacing Ca by Sr. Thus we are able to confirm the Ca/Sr ratio of our sample to be 1:1 as derived from the c -axis parameters. Moreover we are able to localize Ca2 close to a nominal Sr site. The deviation is less than the difference of the ionic radii: $\text{Ca}^{2+} = 1 \text{ \AA}$, $\text{Sr}^{2+} = 1.18 \text{ \AA}$.

3.3 Cu–O dimpling angle

The structural complexity of the Bi-cuprates arises from the unconventional chemical bonding of Bi^{3+} in the doping block. The largely distorted oxygen coordination of Bi reduces the symmetry of the crystal and introduces a structural modulation along the a -axis. Every 5 Bi rows an extra oxygen is introduced into the Bi–O slab which splits apart two Bi atoms. The periodic insertion of extra oxygens in the bridging position results in a periodic bending of the slab and an sinusoidal displacive modulation of all layers [18, 14]. EXAFS is unable to probe directly these long-range modulations [17], but it is rather sensitive to possible short-range modulations. However, the long-range modulation of the apical oxygen in Bi2212 has been recently determined indirectly by polarized EXAFS and found to be rather rectangular than sinusoidal [19, 20].

The forward scattering configurations #12 and #15 in Fig. 1 show the relatively strong multiple scattering in the CuO_2 plane. Although the sum of these contributions is reduced by destructive interferences, it still overshoots the experimental data around 3.4 \AA . A reasonable fit to the peak around 3.4 \AA could be only obtained by

moving the planar oxygens O1 by $z = -0.125 \text{ \AA}$ out of the Cu-plane, which results in a local dimpling angle of 3.5° .

Fig. 2 (*bottom*) displays a fit to the experimental data at 280 K, which turns out to be less satisfactorily than that at 40 K. Here the geometry was only slightly corrected for (admittedly unrealistic isotropic) thermal expansion, and σ_{Cu-O}^2 was increased from 0.0043 \AA^2 to 0.0057 \AA^2 , σ_{Cu-Sr}^2 from 0.007 \AA^2 to 0.01 \AA^2 , and $\sigma_{Cu-Ca1,Ca2}^2$ from 0.006 \AA^2 to 0.008 \AA^2 . The resulting calculation still overshoots the experimental data around 3.4 \AA , but a further increase of the dimpling angle and variations of σ^2 could not improve the fit.

Note also the significant deviations in the single scattering regions $R < 3 \text{ \AA}$, which point to a temperature induced distortion of the local cluster. In particular poor agreement is obtained in the shell of the apical oxygen and the interfering Ca1,2 (#2,3,4 in Fig. 1). We conclude a fit to the temperature dependent data has to be based on a model describing more precisely the temperature induced variations of the polarizable layer than hitherto worked out.

4. Concluding remarks

We have explored the potential of the x-ray extended-absorption fine-structure method for the measurement of the local structure around Cu in $\text{Bi}_2\text{Sr}_{1.5}\text{Ca}_{1.5}\text{Cu}_2\text{O}_8$ using a full multiple-scattering approach. We could determine the Ca/Sr ratio, the Ca2 site, and the Cu–O1 dimpling angle at 40 K. The temperature dependence of the local structure in the polarizable layer has turned out to be rather complex and remains unresolved; further work on this problem is in progress.

Acknowledgements

Special thanks to T. Orgelmacher, Dpt. of Informatics, U Paderborn, for his selfless computational help.

Figure captions

Fig. 1. *Top:* Modulus of the Fouriertransform, $|\text{FT}(\chi k^2)|$, of the Cu-K EXAFS of $\text{Bi}_2(\text{SrCa})_3\text{Cu}_2\text{O}_{8+\delta}$ at 40 K. Thick drawn out line: experimental data. Dashed line: multiple scattering calculation from parameters in Tab. 1, see 'Ca/Sr = 1.5 : 1.5, flat Cu-O1' in Fig. 2. *Below:* Contributions (1–18) of 15 relevant scattering configurations. Oscillating drawn out lines and dashed lines are real and imaginary parts of FT, respectively. Note the strong multiple configurations #12 and #15. No refinement was made for the apical oxygen O2, #2.

Fig. 2. Experimental (drawn out lines) and calculated $|\text{FT}(\chi k^2)|$ (dashed lines) of the Cu-K EXAFS of Bi 2212. *From top to bottom:* Sr and Ca at their nominal sites (2:1) and O1 at $z = -0.125 \text{ \AA}$ off the Cu-plane; one Ca atom close to a nominal Sr site (1.5:1.5), and O1 in the Cu-Plane; one Ca atom close to a nominal Sr site (1.5:1.5), and O1 at $z = -0.125 \text{ \AA}$ off the Cu-plane. *bottom:* Fit to the experimental data at 280 K. Same geometry as above at 40 K, but corrected for thermal expansion. σ^2 are increased. See text.

References

- [1] K.A. Müller. *Materials Chemistry and Physics* **33**, 171 (1993).
- [2] K.A. Müller. *Z. Phys. B* **80**, 193 (1990).
- [3] D. Zech, H. Keller, K. Conder, E. Kaldis, E. Liarokapis, N. Poulakis and K.A. Müller. *Nature* **371**, 681 (1994).
- [4] H. Eschrig and S.-L. Drechsler. *Physica C* **173**, 80 (1991).
- [5] J. Mustre de Leon, J. Batistic, A.R. Bishop, S.D. Conradson and S.A. Trugman. *Phys. Rev. Lett.* **68**, 3236 (1992).
- [6] E.A. Stern, M. Qian, Y. Yacoby, S.M. Heald and H. Maeda. *Physica C* **209**, 331 (1993).
- [7] J. Röhler. Evidence from EXAFS for an axial oxygen centered lattice instability in $\text{YBa}_2\text{Cu}_3\text{O}_{7-\delta}$? In *Materials and Crystallographic Aspects of High T_c -Superconductivity*, Edited by E. Kaldis, volume E 263 of *NATO ASI Series*, p. 353, Kluwer Academic Publishers, Dordrecht, 1994.
- [8] H. Schwer, J. Karpinski and E. Kaldis. Structural low temperature phase transitions in $\text{Y}_x\text{Ca}_{1-x}\text{Ba}_2\text{Cu}_4\text{O}_8$ single crystals. Result of the Spin Gap Opening? Proc. M²S-HTSC IV, Grenoble, France, 5-9 July 1994, in press, 1995.
- [9] P. Majewski. *Adv. Mat.* **6**, 460 (1994).
- [10] J. Röhler and A. Larisch. Evidence for Jahn-Teller Distortions in Bi-Sr-Ca-Cu-O High- T_c Superconductors. In *Electronic Properties of High- T_c Superconductors and Related Compounds*, Edited by H. Kuzmany, J. Fink and M. Mehring, volume 99 of *Springer Series of Solid State Sciences*, p. 152. Springer, Berlin, 1990.
- [11] A. Waldorf. Diplomarbeit, Universität zu Köln, 1990.
- [12] M. Yoshida. *Jap. J. Appl. Phys.* **27**, L2044 (1988).
- [13] P. Bordet, J.J. Capponi, C. Chailout, J. Chenavas, A.W. Hewat, E.A. Hewat, J.L. Hodeau, M. Marezio, J.L. Tholence and D. Tranqui. *Physica C* **189**, 189 (1988).
- [14] A.I. Beskrovnyi, M. Dlouhá, Z. Jiráček, S. Vratislav and E. Pollert. *Physica C* **166**, 79 (1990).
- [15] J.J. Rehr, R.C. Albers and S.I. Zabinsky. *Phys. Rev. Lett.* **69**, 3397 (1992).
- [16] V. Fritzsche. *J. Phys.: Condensed Matter* **2**, 9735 (1990).

- [17] R. Crüsemann. Dissertation, Bayerische Julius-Maximilians-Universität Würzburg, 1993.
- [18] J.M. Tarascon, Y. LePage, W.R. Mc Kinnon, E. Tselepis, P. Barboux, B.G. Bagley and R. Ramesh. On the origin of the structural modulation in the Bi cuprates as derived from 3d-metal substituted phases. In *High Temperature Superconductors: Relationships Between Properties, Structure, and Solid-State Chemistry*, Edited by J.D. Jorgensen, K. Kitazawa, J.M. Tarascon, M.S. Thompson and J.B. Torrance, volume 156 of *Materials Research Society Symposium Proceedings*, p. 317, 9800 McKnight Road, Pittsburgh, Pennsylvania 15237 (U.S.A), 1989. Materials Research Society.
- [19] M. Missori, A. Bianconi, H. Oyanagi and H. Yamaguchi. Evidence for local lattice instability at $T^* \simeq 1.4T_c$ in Bi2212 by EXAFS. Proc. M²S-HTSC IV, Grenoble, France, 5-9 July 1994, in press, North-Holland, Amsterdam, 1995.
- [20] A. Bianconi. These proceedings.

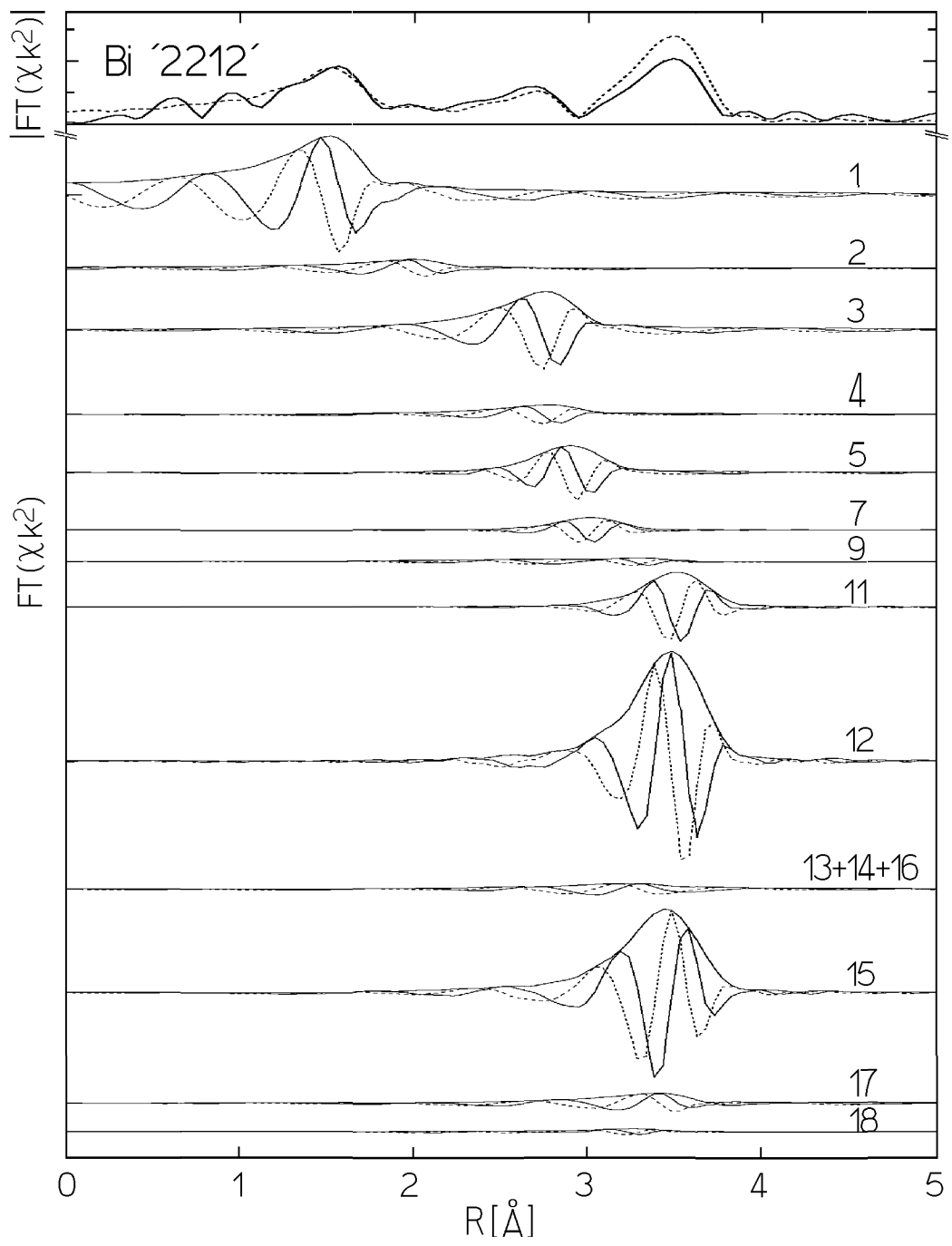


Fig. 1.

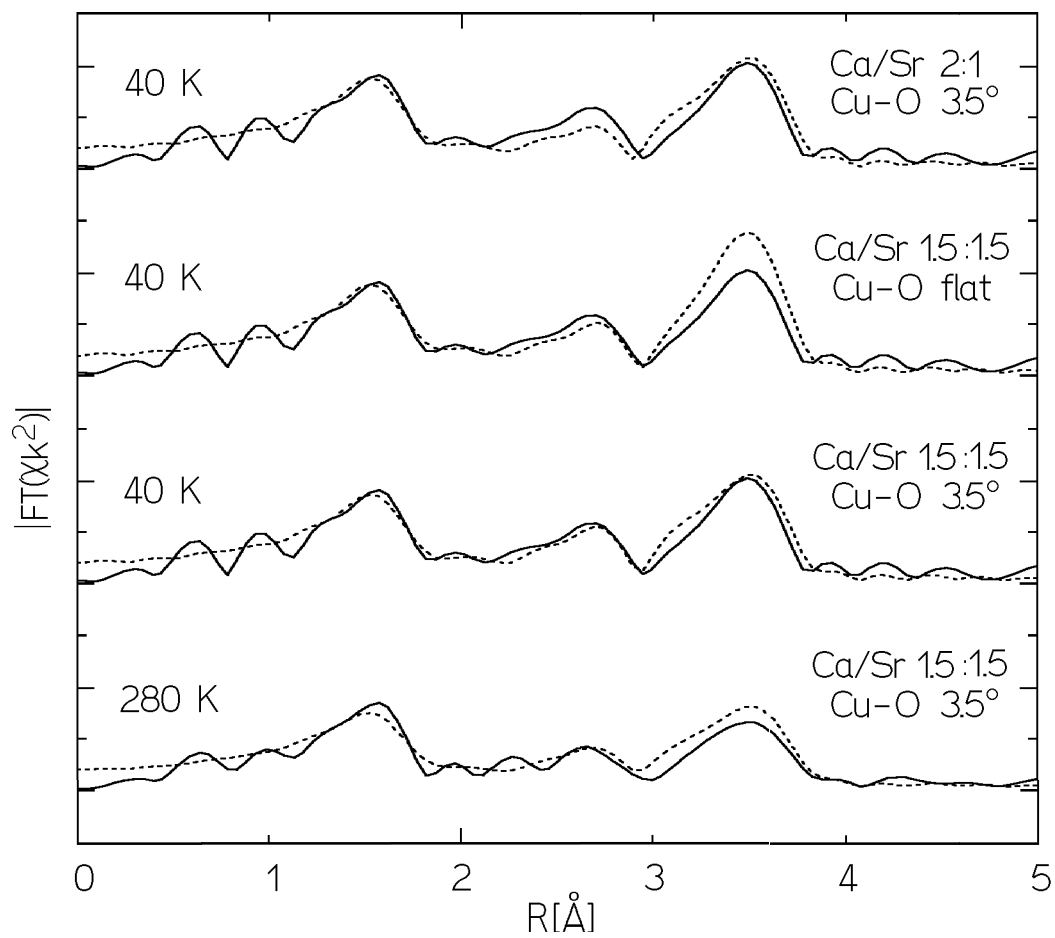


Fig. 2.